Smale Horseshoe via the Anti-integrability

Yi-Chiuan Chen
Institute of Mathematics, Academia Sinica, Taipei 11529, Taiwan
Email: YCChen@math.sinica.edu.tw

25 April 2005

Abstract

The embedding of the Bernoulli shift into the horseshoe map can be viewed as it is inherited from the anti-integrable limit where the horseshoe has infinite contraction in one direction and infinite expansion in the other. At the limit the map is virtually a subshift of finite type with four symbols or equivalently a full shift with two symbols. We present an algebraic explanation for the equivalence of the two shifts.

Key words: Smale's horseshoe, symbolic dynamics, anti-integrable limit, chaos

2000 Mathematics Subject Classification: 37B10, 37D20

1 Introduction

A noteworthy fact is that a dynamical system can be proved to be chaotic if the Smale horseshoe can be embedded in as a subsystem [1, 2, 3]. In addition to the chaoticity, the horseshoe implies the system is conjugate to the Bernoulli shift with two symbols. In oder to identify whether a horseshoe structure exists in a certain region of the phase space, sophisticated geometrical arguments are usually involved. In contrast, the novel theory of anti-integrability provides an analytical method to prove existence of chaotic orbits for dynamical systems. This alternative method also gives a vivid picture on how symbolic dynamics is admitted by a system. In the seminal paper [4], Aubry and Abramovici brought in the concept of anti-integrable limit so as to investigate the standard map. They showed the map essentially reduces to a symbolic dynamical system at the limit, that is, orbits at the limit, called the "anti-integrable orbits", form a Bernoulli shift on the space of sequences. Furthermore, for systems near the anti-integrable limit, their results showed that there are orbits which are also 'near' the anti-integrable ones. By 'near' we mean two orbits $\{(x_i, y_i)\}$ and $\{(\hat{x}_i, \hat{y}_i)\}$ are close to each other in the sense of the uniform topology, i.e. points (x_i, y_i) and $(\hat{x}_i, \hat{y}_i)$ are close to each other in the Euclidean space for every integer i.

This concept has been extended and applied to various systems. Many fruitful results were achieved, such as the existence of invariant cantori for symplectic maps [5], the existence of breathers for time-reversible networks of coupled oscillators [6], the existence of multi-bump trajectories in time-dependent Lagrangian systems [7, 8], and the embedding of symbolic dynamics into the Sinai billiards [9], the logistic maps [10] and into non-autonomous maps [11].

In [12], the anti-integrable limit for the Hénon map [13, 14, 15]

$$(x, y) \mapsto (-a + y + x^2, -bx) \tag{1}$$

at $a \to \infty$ was established, and the explicit Devaney-Nitecki parameter region [16],

$$b \neq 0 \quad \text{and} \quad a > \frac{5 + 2\sqrt{5}}{4}(1 + |b|)^2,$$

for which all nonwandering orbits form a hyperbolic horseshoe, was also obtained in [17] by using the contracting mapping argument. Figure 1 depicts the image

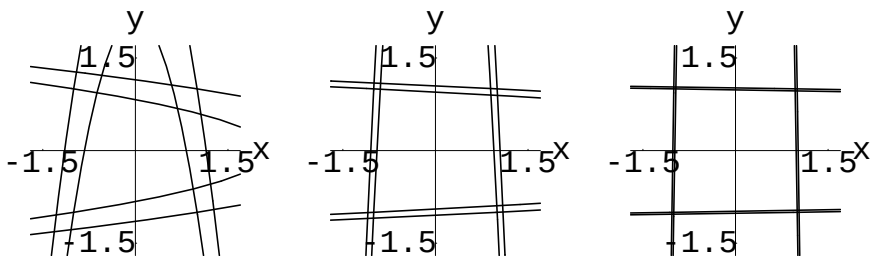

Figure 1: The Hénon family $H_{a,1}$ (from right to left $a = 10$, 100 and 1000).

and pre-image of domain $[-1, 1] \times [-1, 1]$ for an area-preserving Hénon map of the form

$$H_{a,b}(x, y) = (\sqrt{a}(1 - x^2) - by, x) \tag{2}$$

for three values of a. We emphasize that the two maps (1) and (2) are equivalent by the transformation $(x, y) \mapsto (-\sqrt{a}x, \sqrt{a}by)$ only if both a and b are non-zero and of finite value.

One of the prime objectives of this paper is to show that the Smale horseshoe map itself in fact exhibits the anti-integrability. As a consequence, the anti-integrability of the Hénon map $H_{a,b}$ can be correlated with that of the Smale horseshoe. We show the dynamics of a horseshoe which has uniformly contraction rate ϵ and expansion rate $1/\epsilon$ behaves the same as that of figure 1: the limit $\lim_{a\to\infty} H_{a,b}$ corresponds to the limit $\epsilon \to 0$. Similarly, the behaviour of the Lozi map and the Hénon-Lozi-type map studied in [18] for sufficiently large a can be understood in the same manner.

In section 2, we recall the horseshoe map and point out a fact that the map is also conjugate to a subshift of finite type with four symbols defined in figure 3(a), which indeed is conjugate to the full shift on two symbols. We present two methods to prove this fact. The one presented in section 3 is in spirit similar to the ternary expansion used by Banks and Dragan [19], while the other located in section 5 is based on the viewpoint of anti-integrable limit and is going to offer a lucid picture for the conjugacy between the horseshoe map and the subshift in figure 3(a). These two proofs will also deliver an algebraic and analytical insight into how the dynamics passes to the anti-integrable limit. Although the horseshoe map that we consider in section 2 is locally linear and has constant

contraction and expansion rates, our results can be extended to its any C^1-perturbation and to the one with contraction rate ϵ and expansion rate C/ϵ for any non-zero C. In section 4, a review of the anti-integrable limit is presented.

2 Smale horseshoe

Let $1/2 > \epsilon > 0$. Consider a typical case of horseshoe map f_ϵ which shrinks the unit square Q vertically by a factor ϵ and stretches it horizontally by a factor $1/\epsilon$ then bends it back as shown in figure 2. Choose the corner point A to be

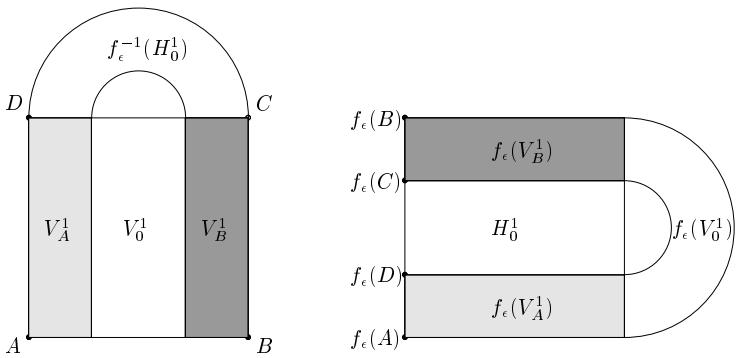

Figure 2: Points A, B, C, D are the four vertices of the square Q and have coordinates $(0,0)$, $(1,0)$, $(1,1)$, $(0,1)$, respectively.

the origin, then on domain Q we can write the diffeomorphism f_ϵ as

$$f_\epsilon(x,y) = \begin{cases} (\frac{x}{\epsilon}, \epsilon y) & \text{if } x \in [0,\epsilon] \\ (\frac{1}{\epsilon} - \frac{x}{\epsilon}, 1-\epsilon y) & \text{if } x \in [1-\epsilon, 1], \end{cases} \tag{3}$$

and its inverse f_ϵ^{-1} as

$$f_\epsilon^{-1}(x,y) = \begin{cases} (\epsilon x, \frac{y}{\epsilon}) & \text{if } y \in [0,\epsilon] \\ (1-\epsilon x, \frac{1}{\epsilon} - \frac{y}{\epsilon}) & \text{if } y \in [1-\epsilon, 1]. \end{cases} \tag{4}$$

It has been known since the work of Smale [1] that the set Λ_ϵ of points whose iterations (both forward and backward under f_ϵ) stay in Q, given by

$$\Lambda_\epsilon = \bigcap_{n\in\mathbb{Z}} f_\epsilon^n(Q),$$

is a Cantor set and that f_ϵ restricted to Λ_ϵ is topologically conjugate to the full two-sided shift with two symbols. In other words, any sequence $\{s_i\}_{i\in\mathbb{Z}}$ with $s_i = A$ or B corresponds to a unique point (x, y) in Λ_ϵ such that $f_\epsilon^i(x, y) \in V_{s_i}^1$ for every integer i.

The formulae for x between ϵ and $1-\epsilon$ in (3) and for y between ϵ and $1-\epsilon$ in (4) are inessential because a point having such an x- or y-coordinate would be mapped outside Q, thus cannot be invariant. Nonetheless, we may choose the image of V_0^1 and the inverse image of H_0^1 to be the semi-annuli of width ϵ as shown in figure 2. We can also extend the horseshoe map to an ambient domain containing Q so that on which f_ϵ is a C^∞-diffeomorphism. For more detailed accounts of the extension and the standard proof of Smale's results, see e.g., textbooks by Robinson [20] or Wiggins [21].

The invariant set Λ_ϵ lies in four disjoint squares, namely in $(V_A^1 \cup V_B^1) \cap f_\epsilon(V_A^1 \cup V_B^1)$, thus it appears that the dynamics of the horseshoe map on Λ_ϵ would have a better fit with our intuition if it is a symbolic dynamics with four symbols. Denoting the four squares by $Q_A^1 \ni A$, $Q_B^1 \ni B$, $Q_C^1 \ni C$ and $Q_D^1 \ni D$ as depicted in figure 4, we show in the next section that the restriction of f_ϵ to Λ_ϵ is topologically conjugate to the subshift $\widetilde{\sigma}$ shown in figure 3.

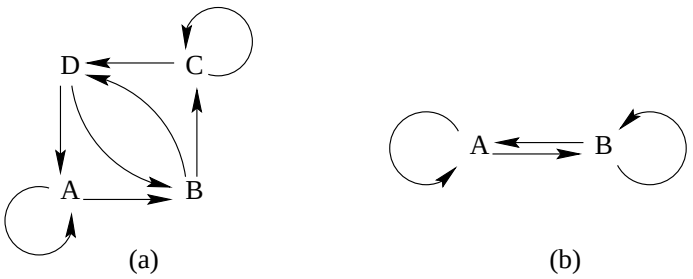

Figure 3: (a) A subshift of finite type $\widetilde{\sigma}$ with four symbols and (b) the full shift with two symbols represented by Markov graphs.

Both shifts in figure 3 have positive topological entropy, $\ln 2$. In fact, these two are equivalent as follows. The shift in (a) reduces to the one in (b) simply by identifying D with A and C with B. Conversely, any sequence $\{s_i\}_{i\in\mathbb{Z}}$ consisting of symbols A or B can be transformed to a unique sequence of A, B, C and D by the following rule:

- if $\{s_i\}$ has words $\{BA\}$, then replace the A by D;

- if $\{s_i\}$ has words $\{BB\}$, then replace the second B by C.

For example, a word $\{AABBA\}$ is transformed to $\{AABCD\}$ or $\{DABCD\}$.

We give two proofs that the dynamics of f_ϵ on Λ_ϵ is as the Markov chain in figure 3(a). The one presented in the next section is algebraical, while the other in section 5 is analytical and is based on an observation that f_ϵ has an anti-integrable limit $\epsilon \to 0$.

3 Symbolic dynamics

To start with, suppose

$$\bigcap_{n=-1}^{1} f_\epsilon^n(Q) = Q^1$$

consists of four components Q_A^1, Q_B^1, Q_C^1 and Q_D^1 as shown in figure 4, and let

$$Q^N = \bigcap_{n=-N}^{N} f_\epsilon^n(Q), \quad N \geq 1,$$

be the set of 4^N squares of area ϵ^{2N} such that $f_\epsilon^{\pm k}(Q^N) \subset Q^{N-k}$ for $0 \leq k < N$. Let $\mathcal{C}(Q^N)$ denote the set of the 4^{N+1} corner points of Q^N, then it is known,

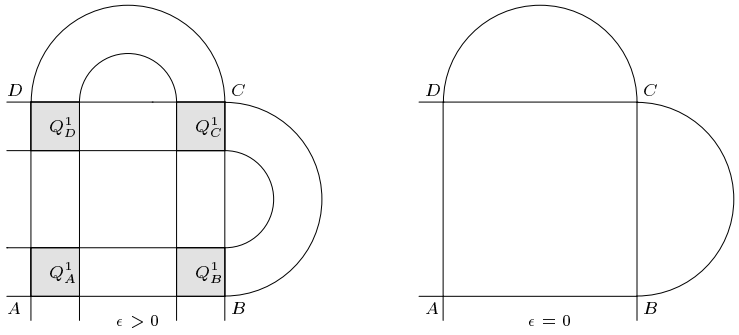

Figure 4: When $\epsilon \to 0$, the four partitions Q_A^1, Q_B^1, Q_C^1 and Q_D^1 collapse to points A, B, C and D, respectively. Note that the horseshoe map is not well-defined and not invertible when $\epsilon = 0$.

e.g. [20, 21, 22], that

$$\Lambda_\epsilon = \lim_{N\to\infty} Q^N \supset \bigcup_{N\geq 0} \mathcal{C}(Q^N) = \lim_{N\to\infty} \mathcal{C}(Q^N)$$

and that Λ_ϵ contains no interior points. Besides, any corner point (x, y) of Q^N has coordinates

$$\begin{aligned} x &= \sum_{k=0}^{N-1} \alpha_k (1-\epsilon)\epsilon^k + \alpha_N \epsilon^N, \\ y &= \sum_{k=-N+1}^{0} \beta_k (1-\epsilon)\epsilon^{|k|} + \beta_{-N}\epsilon^N \end{aligned}$$

with α_k, α_N, β_k, $\beta_{-N} \in \{0, 1\}$. (A reason why we assign negative indices to $\{\beta_k\}$ is because the horseshoe map expands in y-direction when iterates backwards.) Passing to the limit $N \to \infty$ and using the identity $\sum_{k=N}^{\infty}(1-\epsilon)\epsilon^k = \epsilon^N$, we see that any point in Λ_ϵ has coordinates

$$(x, y) = (\sum_{k=0}^{\infty} \alpha_k (1-\epsilon)\epsilon^k, \sum_{k=-\infty}^{0} \beta_k (1-\epsilon)\epsilon^{|k|}), \quad \alpha_k,\ \beta_k \in \{0, 1\}. \tag{5}$$

(Notice that the expression above is the ternary expansion when $\epsilon = 1/3$, e.g. [19, 20].) Hence,

$$(x, y) \in \begin{cases} Q_A^1 \\ Q_B^1 \\ Q_C^1 \\ Q_D^1 \end{cases} \quad \text{iff} \quad (\alpha_0, \beta_0) = \begin{cases} (0,0) \\ (1,0) \\ (1,1) \\ (0,1). \end{cases} \tag{6}$$

For any $(x, y) \in \Lambda_\epsilon$, some calculation by making use of formula (3) shows that

$$f_\epsilon(x, y) = \begin{cases} (\sum\limits_{k=1}^{\infty} \alpha_k (1-\epsilon)\epsilon^{k-1}, \sum\limits_{k=-\infty}^{-1} \beta_{k+1}(1-\epsilon)\epsilon^{|k|}) & \text{if } \alpha_0 = 0 \\ (\sum\limits_{k=0}^{\infty} \overline{\alpha}_{k+1}(1-\epsilon)\epsilon^k, 1-\epsilon+\sum\limits_{k=-\infty}^{-1} \overline{\beta}_{k+1}(1-\epsilon)\epsilon^{|k|}) & \text{if } \alpha_0 = 1, \end{cases} \tag{7}$$

where $\overline{\alpha}_k = 1 - \alpha_k$ and $\overline{\beta}_k = 1 - \beta_k$. In the light of (6), we get

$$f_\epsilon(x, y) \in \begin{cases} Q_A^1 \\ Q_B^1 \\ Q_C^1 \\ Q_D^1 \end{cases} \quad \text{iff} \quad (\alpha_0, \alpha_1) = \begin{cases} (0,0) \\ (0,1) \\ (1,0) \\ (1,1). \end{cases} \tag{8}$$

Combining (6) and (8), we infer that the Markov chain between partitions Q_A^1, Q_B^1, Q_C^1 and Q_D^1 must look like that of figure 3(a), as claimed in the Introduction section.

The Markov graph for inverse map of f_ϵ can be obtained simply by reversing direction of the arrows in figure 3(a), or by observing the following facts:

$$f_\epsilon^{-1}(x,y) = \begin{cases} (\sum\limits_{k=1}^{\infty} \alpha_{k-1}(1-\epsilon)\epsilon^k, \sum\limits_{k=-\infty}^{0} \beta_{k-1}(1-\epsilon)\epsilon^{|k|}) & \text{if } \beta_0 = 0 \\ (1-\epsilon+\sum\limits_{k=1}^{\infty} \overline{\alpha}_{k-1}(1-\epsilon)\epsilon^k, \sum\limits_{k=-\infty}^{0} \overline{\beta}_{k-1}(1-\epsilon)\epsilon^{|k|}) & \text{if } \beta_0 = 1, \end{cases} \tag{9}$$

and

$$f_\epsilon^{-1}(x,y) \in \begin{cases} Q_A^1 \\ Q_B^1 \\ Q_C^1 \\ Q_D^1 \end{cases} \quad \text{iff} \quad (\beta_0,\beta_{-1}) = \begin{cases} (0,0) \\ (1,1) \\ (1,0) \\ (0,1). \end{cases} \tag{10}$$

An easier way to look at formulae (7) and (9) is via the map H defined below. The idea of introducing H is adapted from the enlightening works [19, 23].

Let Σ_2 be the space of sequences of 0's and 1's,

$$\Sigma_2 := \{(\cdots \beta_{-2}\beta_{-1}, \beta_0\alpha_0, \alpha_1\alpha_2 \cdots) | \quad \alpha_i,\ \beta_i = 0 \text{ or } 1\ \forall\ i\},$$

then there is a one to one correspondence between Σ_2 and Λ_ϵ because of (5). We define the map H on Σ_2 as follows:

$$H(\cdots \beta_{-2}\beta_{-1}, \beta_0\alpha_0, \alpha_1\alpha_2 \cdots) = \begin{cases} (\cdots \beta_{-1}\beta_0, \alpha_0\alpha_1, \alpha_2\alpha_3 \cdots) \\ (\cdots \overline{\beta}_{-1}\overline{\beta}_0, \alpha_0\overline{\alpha}_1, \overline{\alpha}_2\overline{\alpha}_3 \cdots) \end{cases} \quad \text{if } \alpha_0 = \begin{cases} 0 \\ 1. \end{cases} \tag{11}$$

The map is invertible, and its inverse reads

$$H^{-1}(\cdots \beta_{-2}\beta_{-1}, \beta_0\alpha_0, \alpha_1\alpha_2 \cdots) = \begin{cases} (\cdots \beta_{-3}\beta_{-2}, \beta_{-1}\beta_0, \alpha_0\alpha_1 \cdots) \\ (\cdots \overline{\beta}_{-3}\overline{\beta}_{-2}, \overline{\beta}_{-1}\beta_0, \overline{\alpha}_0\overline{\alpha}_1 \cdots) \end{cases} \quad \text{if } \beta_0 = \begin{cases} 0 \\ 1. \end{cases} \tag{12}$$

So, the map H is an alternative way to describe the horseshoe map on Λ_ϵ.

Let Σ_4 be the space of sequences consisting of four symbols A, B, C and D, and $\widetilde{\Sigma}_4 := \widetilde{\sigma}|\Sigma_4$ the subspace of Σ_4 in which a sequence of symbols being admissible is in accordance with the Markov chain given in figure 3(a). Then each point in Σ_2 determines a unique point in $\widetilde{\Sigma}_4$ and vice versa, by means of (6), (8), (10), (11) and (12). For example, the point

$$(\cdots 0, 00, 1011000 \cdots)$$

corresponds to

$$(\cdots A, A, BCCDBDA\cdots).$$

The following commutative diagram verifies the example just mentioned:

$$\begin{array}{ccc}
\vdots\uparrow & & \uparrow\vdots \\
(\cdots, 00, 01011000\cdots) & \overset{\text{by (6)}}{\longrightarrow} & (\cdots, A, ABCCDBDA\cdots) \\
{\scriptstyle H^{-1}}\uparrow & & \uparrow{\scriptstyle \sigma^{-1}} \\
(\cdots 0, 00, 1011000\cdots) & \overset{\text{by (6)}}{\longrightarrow} & (\cdots A, A, BCCDBDA\cdots) \\
{\scriptstyle H}\downarrow & & \downarrow{\scriptstyle \sigma} \\
(\cdots 00, 01, 011000\cdots) & \overset{\text{by (6)}}{\longrightarrow} & (\cdots AA, B, CCDBDA\cdots) \\
{\scriptstyle H}\downarrow & & \downarrow{\scriptstyle \sigma} \\
(\cdots 111, 11, 00111\cdots) & \overset{\text{by (6)}}{\longrightarrow} & (\cdots AAB, C, CDBDA\cdots) \\
{\scriptstyle H}\downarrow & & \downarrow{\scriptstyle \sigma} \\
(\cdots 0000, 11, 1000\cdots) & \overset{\text{by (6)}}{\longrightarrow} & (\cdots AABC, C, DBDA\cdots) \\
{\scriptstyle H}\downarrow & & \downarrow{\scriptstyle \sigma} \\
(\cdots 11110, 10, 111\cdots) & \overset{\text{by (6)}}{\longrightarrow} & (\cdots AABCC, D, BDA\cdots) \\
\vdots\downarrow & & \downarrow\vdots\ .
\end{array}$$

The above investigation clearly indicates that the Smale horseshoe f_ϵ on the invariant set Λ_ϵ can be described in more detail by conjugating it with the subshift $\widetilde{\sigma}$ as in figure 3(a) than with the full shift in figure 3(b). The one-to-one correspondence between the two spaces $\widetilde{\Sigma}_4$ and Σ_2 can be shown to be a homeomorphism if both spaces are equipped with the product topology, then the conjugacy between f_ϵ and $\widetilde{\sigma}$ can be proved. We do not intend to give the detail of the proof since it can be obtained by copying the standard procedure (see e.g. [20, 21]) with mild modification. Instead, we present another proof whose procedure is in spirit of the so-called anti-integrability.

4 Conjugacy via the anti-integrability

The following definition originates from the nice review [12] and is re-written to fit the current context.

Definition 4.1. *A one-parameter family of C^1-diffeomorphisms f_ϵ of $\mathbb{R}^n$*

$$z_{i+1} = f_\epsilon(z_i), \quad i \in \mathbb{Z}, \tag{13}$$

is called "anti-integrable" when $\epsilon \to 0$ *if*

1. *there exists a family of functions* $L_\epsilon : \mathbb{R}^n \times \mathbb{R}^n \to \mathbb{R}^n$ *such that the equation*

$$L_\epsilon(z_i, z_{i+1}) = 0 \tag{14}$$

   is equivalent to (13) for nonzero ϵ *and such that the limit*

$$\lim_{\epsilon \to 0} L_\epsilon(z_i, z_{i+1}) = L_0(z_i, z_{i+1})$$

   exists and is independent of z_{i+1}*;*

2. *the set of solutions* $\{z_i\}$ *of* $L_0(z_i, z_{i+1}) = 0$ *for all* i *can be characterized bijectively by a subset of* $\mathfrak{S}^{\mathbb{Z}}$ *of infinite sequences with* $\mathfrak{S}$ *being a certain finite set.*

The limit $\epsilon \to 0$ is called the "anti-integrable limit" at which the map f_ϵ (13) loses its dynamics since (14) becomes an algebraic equation. We call a sequence $\{z_i\}$ comprising the solutions of $L_0(z_i, z_{i+1}) = 0$ for all i an "anti-integrable orbit" or "anti-integrable solution" of the map f_0.

The significance of the anti-integrable limit is as follows. Endow the set $\mathfrak{S}$ with the discrete topology and the set $\mathfrak{S}^{\mathbb{Z}}$ with the product topology. If the set $\widetilde{\Sigma}$ of sequences formed by the anti-integrable orbits is in fact continuously dependent upon a closed subset of $\mathfrak{S}^{\mathbb{Z}}$, then $\widetilde{\Sigma}$ is a compact set in the product space $(\mathbb{R}^n)^{\mathbb{Z}}$. Furthermore, if the subset of $\mathfrak{S}^{\mathbb{Z}}$ is an irreducible subshift of finite type, then $\widetilde{\Sigma}$ is a Cantor set. Therefore, at the anti-integrable limit, the system is virtually a subshift with $\#(\mathfrak{S})$ symbols. ($\#(\mathfrak{S})$ is the cardinality of the set $\mathfrak{S}$.)

For example, suppose the discrete set $\mathfrak{S}$ is $\{A, B\}$ and suppose any anti-integrable orbit corresponds to a unique element in the set $\{A, B\}^{\mathbb{Z}}$ and vice versa. Then the map at the anti-integrable limit is the Bernoulli shift of the two symbols A and B, and therefore has positive topological entropy.

For sufficiently smooth maps satisfying some non-degeneracy condition, the theory of anti-integrability says that the embedded symbolic dynamics persists to small perturbations. Let $l_\infty := \{\mathbf{z} |\ \mathbf{z} = \{z_i\},\ i \in \mathbb{Z}\}$ endowed with the sup norm be the Banach space of bounded sequences in $\mathbb{R}^n$. Define a map $F : l_\infty \times \mathbb{R} \to l_\infty$ by

$$F(\mathbf{z}, \epsilon) = \{F_i(\mathbf{z}, \epsilon)\}_{i \in \mathbb{Z}}$$

with

$$F_i(\mathbf{z}, \epsilon) = L_\epsilon(z_i, z_{i+1}),$$

then the theory can be formulated by several steps [4, 5, 11].

1. A bounded anti-integrable orbit $\mathbf{z}^\dagger$ is such that $F(\mathbf{z}^\dagger, 0) = 0$.

2. Let $\widetilde{\Sigma} \subset (\mathbb{R}^n)^{\mathbb{Z}}$ be the set constituting all such $\mathbf{z}^\dagger$'s in step 1, then $\widetilde{\Sigma}$ with the product topology is a Cantor set if $\widetilde{\Sigma}$ is continuously bijective to an irreducible subset of $\mathfrak{S}^{\mathbb{Z}}$ (since an irreducible subset set of $\mathfrak{S}^{\mathbb{Z}}$ is a Cantor set [20]).

3. If $F(\mathbf{z}, \epsilon)$ is C^1 in a neighbourhood of $(\mathbf{z}^\dagger, 0)$ (it is the case if $L_\epsilon(z_i, z_{i+1})$ depends jointly C^1 on its parameter and variables) and if the differential map

$$\begin{aligned} D_{\mathbf{z}} F(\mathbf{z}^\dagger, 0) : l_\infty &\rightarrow l_\infty, \\ \xi := \{\xi_i\}_{i\in\mathbb{Z}} &\mapsto \left\{ \sum_{j\in\mathbb{Z}} D_{z_j} F_i(\mathbf{z}^\dagger, 0)\xi_j \right\}_{i\in\mathbb{Z}} \end{aligned}$$

   is invertible, then the implicit function theorem implies there exists ϵ_0 and a unique C^1-function

$$\theta(\cdot; \mathbf{z}^\dagger) : \mathbb{R} \rightarrow l_\infty, \qquad \epsilon \mapsto \theta(\epsilon; \mathbf{z}^\dagger)$$

   such that $F(\theta(\epsilon; \mathbf{z}^\dagger), \epsilon) = 0$ and $\theta(0; \mathbf{z}^\dagger) = \mathbf{z}^\dagger$ for $0 \leq |\epsilon| < \epsilon_0$.

4. Suppose the assumptions in step 3 are fulfilled for every $\mathbf{z}^\dagger \in \widetilde{\Sigma}$ and ϵ_0 is independent of $\mathbf{z}^\dagger$. Let the projection $\mathbf{z} = (\cdots, z_{-1}, z_0, z_1, \cdots) \mapsto z_0 \in \mathbb{R}^n$ be denoted by π, then a set $\mathcal{A}_\epsilon$ defined by

$$\mathcal{A}_\epsilon := \bigcup_{\mathbf{z}^\dagger \in \widetilde{\Sigma}} \pi(\theta(\epsilon; \mathbf{z}^\dagger))$$

   is a Cantor in $\mathbb{R}^n$ when $\epsilon \neq 0$ provided $\widetilde{\Sigma}$ is a Cantor set. This is because the composition of mappings

$$\mathbf{z}^\dagger \overset{\Phi_\epsilon}{\longmapsto} \theta(\epsilon; \mathbf{z}^\dagger) \overset{\pi}{\longmapsto} \theta(\epsilon; \mathbf{z}^\dagger)_0$$

   is a continuous bijection with the product topology. The fact that Φ_ϵ is continuous is proven in Lemma 4.2 below. π, which is certainly continuous, is bijective since the orbit $\theta(\epsilon; \mathbf{z}^\dagger)$ is uniquely determined by its initial point $\theta(\epsilon; \mathbf{z}^\dagger)_0$ when $\epsilon \neq 0$.

5. The following diagram commutes when $0 < |\epsilon| < \epsilon_0$.

$$\begin{array}{ccc} \widetilde{\Sigma} & \xrightarrow{\sigma} & \widetilde{\Sigma} \\ {\scriptstyle \pi\circ\Phi_\epsilon}\downarrow & & \downarrow{\scriptstyle \pi\circ\Phi_\epsilon} \\ \mathcal{A}_\epsilon & \xrightarrow{f_\epsilon} & \mathcal{A}_\epsilon \end{array}$$

Verifying this diagram amounts to checking the following identity

$$\theta(\epsilon; \mathbf{z}^\dagger)_1 = \theta(\epsilon; \sigma(\mathbf{z}^\dagger))_0.$$

For every i, as can be seen in Step 3, $\theta(\epsilon; \sigma(\mathbf{z}^\dagger))_i$ is the unique orbit point continued from $\sigma(\mathbf{z}^\dagger)_i$, or equivalently is the unique orbit point continued from $(\mathbf{z}^\dagger)_{i+1}$, thus $\theta(\epsilon; \mathbf{z}^\dagger)_{i+1}$ must be $\theta(\epsilon; \sigma(\mathbf{z}^\dagger))_i$ by the uniqueness. When $\widetilde{\Sigma}$ is a subshift of finite type, the homeomorphism $\pi \circ \Phi_\epsilon$ acts as a conjugacy with which the restriction of f_ϵ to the invariant set $\mathcal{A}_\epsilon$ is topologically conjugate to $\sigma|\widetilde{\Sigma}$.

Lemma 4.2. *The map Φ_ϵ is continuous in the product topology for small ϵ.*

Proof. The implicit function theorem result in Steps 3 and 4 implies that for each $\mathbf{z}^\dagger$ and for $0 \leq |\epsilon| < \epsilon_0$ with ϵ_0 sufficiently small, there is a closed ball $U_{\mathbf{z}^\dagger}$ in l_∞ which contains $\theta(\epsilon; \mathbf{z}^\dagger)$ and the diameter of which is independent of $\mathbf{z}^\dagger$ so that $\Phi_\epsilon(\mathbf{z}^\dagger)$ is the unique fixed point for the contraction map $G(\cdot; \mathbf{z}^\dagger, \epsilon) : \mathbf{z} \mapsto \mathbf{z} - D_{\mathbf{z}} F(\mathbf{z}^\dagger, 0)^{-1} F(\mathbf{z}, \epsilon)$ in $U_{\mathbf{z}^\dagger}$. Therefore, it suffices to show that G or equivalently each component of G depends continuously on $\mathbf{z}^\dagger$ with the product topology.

By our condition on $L_0(z_i, z_{i+1})$ for the anti-integrable limit, $D_{\mathbf{z}} F(\mathbf{z}^\dagger, 0)^{-1}$ is diagonal. So, $G(\mathbf{z}; \mathbf{z}^\dagger, \epsilon)_i = z_i - D_{z_i} L_0(z_i^\dagger, z_{i+1}^\dagger)^{-1} L_\epsilon(z_i, z_{i+1})$. We know that $D_{z_i} L_0(z_i^\dagger, z_{i+1}^\dagger)^{-1}$ depends continuously on $z_i^\dagger$ only, so does $G(\mathbf{z}; \mathbf{z}^\dagger, \epsilon)_i$, and this implies $G(\mathbf{z}; \mathbf{z}^\dagger, \epsilon)_i$ depends continuously on $\mathbf{z}^\dagger$ also. □

5 Application to the horseshoe map

Let $l_\infty = \{(\mathbf{x}, \mathbf{y}) | (\mathbf{x}, \mathbf{y}) = \{(x_i, y_i)\},\ i \in \mathbb{Z}\}$ be the space of bounded sequences in $\mathbb{R}^2$, and let the smooth map $F : l_\infty \times \mathbb{R} \to l_\infty$, $F((\mathbf{x}, \mathbf{y}), \epsilon) =$

$\{L_\epsilon((x_i, y_i), (x_{i+1}, y_{i+1}))\}_{i\in\mathbb{Z}}$, be such that

$$L_\epsilon((x_i, y_i), (x_{i+1}, y_{i+1})) = \begin{cases} (\epsilon x_{i+1} - x_i, y_{i+1} - \epsilon y_i) & \text{if } x_i \in [0, \epsilon] \\ (\epsilon x_{i+1} + x_i - 1, y_{i+1} + \epsilon y_i - 1) & \text{if } x_i \in [1-\epsilon, 1]. \end{cases}$$

Then when $1/2 > \epsilon > 0$, $(\mathbf{x}, \mathbf{y})$ is an orbit of the horseshoe map f_ϵ confined in Q if and only if it solves $F((\mathbf{x}, \mathbf{y}), \epsilon) = 0$. It is readily to see the limit $\lim_{\epsilon\to 0} L_\epsilon((x_i, y_i), (x_{i+1}, y_{i+1}))$ exists and depends on (x_i, y_i) only. The following theorem verifies the second condition of Definition 4.1, thus the horseshoe map f_ϵ is anti-integrable.

Theorem 5.1. *The dynamics of $F((\mathbf{x}, \mathbf{y}), 0) = \mathbf{0}$ is the subshift $\widetilde{\sigma}$ in figure 3.*

Proof. When $\epsilon = 0$, $F((\mathbf{x}, \mathbf{y}), \epsilon) = \mathbf{0}$ reduces to a sequence of algebraic equations with

$$\begin{cases} y_{i+1} = 0 & \text{if } x_i = 0 \\ y_{i+1} = 1 & \text{if } x_i = 1. \end{cases} \tag{15}$$

As a result, if $(x_i, y_i) = (0, 0)$, then (x_{i+1}, y_{i+1}) can be either $(0, 0)$ or $(1, 0)$; if $(x_i, y_i) = (1, 0)$, (x_{i+1}, y_{i+1}) can be $(0, 1)$ or $(1, 1)$; if $(x_i, y_i) = (0, 1)$, (x_{i+1}, y_{i+1}) can be $(0, 0)$ or $(1, 0)$; if $(x_i, y_i) = (1, 1)$, (x_{i+1}, y_{i+1}) can be $(0, 1)$ or $(1, 1)$. The four points $(0, 0)$, $(0, 1)$, $(1, 1)$ and $(1, 0)$ are denoted by A, B, C and D, respectively, therefore the orbits of (15) is nothing but the Markov chain in figure 3(a). □

Denote the set of anti-integrable orbits $(\mathbf{x}^\dagger, \mathbf{y}^\dagger)$, satisfying $F((\mathbf{x}^\dagger, \mathbf{y}^\dagger), 0) = \mathbf{0}$, by $\widetilde{\Sigma}$. The theorem below shows the symbolic dynamics of the horseshoe map can be viewed as it is inherited from the anti-integrable limit.

Theorem 5.2. *Suppose $0 < \epsilon < 1/2$. There exists a smooth family of continuous functions $g_\epsilon : \widetilde{\Sigma} \to \mathbb{R}^2$, parametrized by ϵ, such that $g_\epsilon((\mathbf{x}^\dagger, \mathbf{y}^\dagger))$ is an orbit of the horseshoe map f_ϵ and $g_0((\mathbf{x}^\dagger, \mathbf{y}^\dagger)) = (\mathbf{x}^\dagger, \mathbf{y}^\dagger)$ for any anti-integrable orbit $(\mathbf{x}^\dagger, \mathbf{y}^\dagger)$. Conversely, if $(\mathbf{x}_\epsilon, \mathbf{y}_\epsilon)$ is a horseshoe orbit, then there exists a unique $(\mathbf{x}^\dagger, \mathbf{y}^\dagger)$ such that $(\mathbf{x}_\epsilon, \mathbf{y}_\epsilon) = g_\epsilon((\mathbf{x}^\dagger, \mathbf{y}^\dagger))$. Moreover, the sets defined by $\Lambda_\epsilon := g_\epsilon(\widetilde{\Sigma})$ form a continuous family of Cantor sets, and for a given ϵ, $f_\epsilon|\Lambda_\epsilon$ is topologically conjugate to $\widetilde{\sigma}|\Sigma_4 = \sigma|\widetilde{\Sigma}$.*

Proof. Denote the partial derivative of F with respect to the first variable at $(\mathbf{x},\mathbf{y})$ by $\mathcal{L}_\epsilon(\mathbf{x},\mathbf{y})$, that is,

$$\begin{aligned}\mathcal{L}_\epsilon(\mathbf{x},\mathbf{y}) : l_\infty &\to l_\infty,\\ (\mathbf{u},\mathbf{v}) &\mapsto (\mathbf{w},\mathbf{z}) := \mathcal{L}_\epsilon(\mathbf{x},\mathbf{y})(\mathbf{u},\mathbf{v})\end{aligned}$$

of which the i-th component reads

$$(w_i,z_i) = \begin{cases}(\epsilon u_{i+1} - u_i, v_{i+1} - \epsilon v_i) & \text{if } x_i \in [0,\epsilon]\\ (\epsilon u_{i+1} + u_i, v_{i+1} + \epsilon v_i) & \text{if } x_i \in [1-\epsilon,1].\end{cases} \tag{16}$$

The invertibility of $\mathcal{L}_\epsilon(\mathbf{x}^\dagger,\mathbf{y}^\dagger)$ when $\epsilon = 0$ for every $(\mathbf{x}^\dagger,\mathbf{y}^\dagger)$ belonging to $\widetilde{\Sigma}$ is evident. The implicit function theorem thus implies there exists $\epsilon_0 > 0$ and a unique C^1-function

$$\theta(\cdot;\mathbf{x}^\dagger,\mathbf{y}^\dagger) : [0,\epsilon_0) \to l_\infty, \quad \epsilon \mapsto \theta(\epsilon;\mathbf{x}^\dagger,\mathbf{y}^\dagger),$$

such that $F(\theta(\epsilon;\mathbf{x}^\dagger,\mathbf{y}^\dagger),\epsilon) = 0$, $\theta(0;\mathbf{x}^\dagger,\mathbf{y}^\dagger) = (\mathbf{x}^\dagger,\mathbf{y}^\dagger)$, and that the set $\Lambda_\epsilon := \bigcup_{(\mathbf{x}^\dagger,\mathbf{y}^\dagger)\in\widetilde{\Sigma}} \pi\circ\theta(\epsilon;\mathbf{x}^\dagger,\mathbf{y}^\dagger)$ is a Cantor in $\mathbb{R}^2$ provided $0 < \epsilon < \epsilon_0$. For given ϵ, the homeomorphism $g_\epsilon := \pi\circ\Phi_\epsilon$ hence acts as a conjugacy between f_ϵ and the subshift of finite type $\widetilde{\sigma}$.

For $\epsilon_0 \le \epsilon < 1/2$, we need to show the linear map $\mathcal{L}_\epsilon(\mathbf{x},\mathbf{y})$ is still invertible, or equivalently need to show there exists a unique bounded sequence $\{(u_i,v_i)\}$ solving equation (16) for a given sequence $\{(w_i,z_i)\}$. But, a bounded sequence of the form

$$\{(u_i,v_i)\} = \left\{-\sum_{k=0}^{\infty}\left(\prod_{l=0}^{k} S(x_{i+l})\right)\epsilon^k w_{i+k},\ z_{i-1} + \sum_{k=1}^{\infty}\left(\prod_{l=1}^{k} S(x_{i-l})\right)\epsilon^k z_{i-k-1}\right\},$$

with

$$S(x) = \begin{cases}1 & \text{if } x \in [0,\epsilon]\\ -1 & \text{if } x \in [1-\epsilon,1]\end{cases}$$

is a solution. In addition, this solution is the only bounded one because the homogeneous solution of (16), which has the form

$$\begin{aligned}u_{i+N} &= \left(\prod_{k=0}^{N-1} S(x_{i+k})\right)\epsilon^{-N}u_i,\\ v_{i-N} &= \left(\prod_{k=1}^{N} S(x_{i-k})\right)\epsilon^{-N}v_i,\end{aligned}$$

cannot be bounded unless it is zero.

The proof of the theorem will complete after showing Lemma 4.2 can be extended to $\epsilon < 1/2$.

Lemma 5.3. *The map* $\Phi_\epsilon : (\mathbf{x}^\dagger, \mathbf{y}^\dagger) \mapsto \theta(\epsilon; \mathbf{x}^\dagger, \mathbf{y}^\dagger)$ *is continuous in the product topology if* $\epsilon < 1/2$.

Proof. For each given $(\mathbf{x}^\dagger, \mathbf{y}^\dagger)$, we know by our construction that $\theta(\epsilon; \mathbf{x}^\dagger, \mathbf{y}^\dagger)_i$ lies inside one of the four squares Q_A^1, Q_B^1, Q_C^1 or Q_D^1. Assume $(\bar{\mathbf{x}}^\dagger, \bar{\mathbf{y}}^\dagger) := \{(\bar{x}_i^\dagger, \bar{y}_i^\dagger)\}$ and $(\hat{\mathbf{x}}^\dagger, \hat{\mathbf{x}}^\dagger) := \{(\hat{x}_i^\dagger, \hat{x}_i^\dagger)\}$ both belong to $\widetilde{\Sigma}$, and assume $(\bar{x}_i^\dagger, \bar{y}_i^\dagger) = (\hat{x}_i^\dagger, \hat{x}_i^\dagger)$ for $|i| \le N$ for some positive integer N. When ϵ varies, $\theta(\epsilon; \bar{\mathbf{x}}^\dagger, \bar{\mathbf{y}}^\dagger)$ and $\theta(\epsilon; \hat{\mathbf{x}}^\dagger, \hat{\mathbf{y}}^\dagger)$ form two continuous curves in l_∞, thus $\theta(\epsilon; \bar{\mathbf{x}}^\dagger, \bar{\mathbf{y}}^\dagger)_i$ and $\theta(\epsilon; \hat{\mathbf{x}}^\dagger, \hat{\mathbf{y}}^\dagger)_i$ must belong to the same square for each $|i| \le N$. The linear expansion in x-direction and contraction in y-direction of the horseshoe map then imply, by the mean value theorem, that

$$\begin{aligned} |\theta_x(\epsilon; \bar{\mathbf{x}}^\dagger, \bar{\mathbf{y}}^\dagger)_i - \theta_x(\epsilon; \hat{\mathbf{x}}^\dagger, \hat{\mathbf{y}}^\dagger)_i| &= \epsilon^{-i} |\theta_x(\epsilon; \bar{\mathbf{x}}^\dagger, \bar{\mathbf{y}}^\dagger)_0 - \theta_x(\epsilon; \hat{\mathbf{x}}^\dagger, \hat{\mathbf{y}}^\dagger)_0| \\ |\theta_y(\epsilon; \bar{\mathbf{x}}^\dagger, \bar{\mathbf{y}}^\dagger)_i - \theta_y(\epsilon; \hat{\mathbf{x}}^\dagger, \hat{\mathbf{y}}^\dagger)_i| &= \epsilon^{i} |\theta_y(\epsilon; \bar{\mathbf{x}}^\dagger, \bar{\mathbf{y}}^\dagger)_0 - \theta_y(\epsilon; \hat{\mathbf{x}}^\dagger, \hat{\mathbf{y}}^\dagger)_0| \end{aligned}$$

for $|i| \le N$, where $\theta_x(\epsilon; \bar{\mathbf{x}}^\dagger, \bar{\mathbf{y}}^\dagger)_i$ denotes the x-component of $\theta(\epsilon; \bar{\mathbf{x}}^\dagger, \bar{\mathbf{y}}^\dagger)_i$ and similar notation for the y-component and for the $(\hat{\mathbf{x}}^\dagger, \hat{\mathbf{y}}^\dagger)$ case. Thus, $|\theta(\epsilon; \bar{\mathbf{x}}^\dagger, \bar{\mathbf{y}}^\dagger)_0 - \theta(\epsilon; \hat{\mathbf{x}}^\dagger, \hat{\mathbf{y}}^\dagger)_0| \le C\epsilon^{N+1}$ for some constant C. These lead to

$$|\theta(\epsilon; \bar{\mathbf{x}}^\dagger, \bar{\mathbf{y}}^\dagger)_i - \theta(\epsilon; \hat{\mathbf{x}}^\dagger, \hat{\mathbf{y}}^\dagger)_i| \le \begin{cases} C\epsilon^{N-|i|+1} & \text{if } |i| \le N \\ 1 & \text{if } |i| > N. \end{cases}$$

Suppose the topology is induced by a metric that the distance between $\theta(\epsilon; \bar{\mathbf{x}}^\dagger, \bar{\mathbf{y}}^\dagger)$ and $\theta(\epsilon; \hat{\mathbf{x}}^\dagger, \hat{\mathbf{y}}^\dagger)$ is equal to $\sum_{i \in \mathbb{Z}} 10^{-|i|} |\theta(\epsilon; \bar{\mathbf{x}}^\dagger, \bar{\mathbf{y}}^\dagger)_i - \theta(\epsilon; \hat{\mathbf{x}}^\dagger, \hat{\mathbf{y}}^\dagger)_i|$ and that the distance between $(\bar{\mathbf{x}}^\dagger, \bar{\mathbf{y}}^\dagger)$ and $(\hat{\mathbf{x}}^\dagger, \hat{\mathbf{y}}^\dagger)$ is $\sum_{i \in \mathbb{Z}} 10^{-|i|} |(\bar{\mathbf{x}}_i^\dagger, \bar{\mathbf{y}}_i^\dagger) - (\hat{\mathbf{x}}_i^\dagger, \hat{\mathbf{y}}_i^\dagger)|$, then the above inequality ascertains the map in question is continuous. □

References

[1] Smale S. Differentiable dynamical systems. Bull Amer Math Soc, 1967;73:747-817.

[2] Kennedy J and Yorke JA. Topological horseshoes. Trans Amer Math Soc, 2001;353:2513-2530.

[3] Yang X-S and Tang Y. Horseshoes in piecewise continuous maps. Chaos Solitons Fractals, 2004;19:841-845.

[4] Aubry S and Abramovici G. Chaotic trajectories in the standard map: the concept of anti-integrability. Physica D, 1990;43:199-219.

[5] MacKay RS and Meiss JD. Cantori for symplectic maps near the anti-integrable limit. Nonlinearity, 1992;5:149-160.

[6] MacKay RS and Aubry S. Existence of breathers for time-reversible or Hamiltonian networks of weakly coupled oscillators. Nonlinearity, 1994;7:1623-1643.

[7] Bolotin SV and MacKay RS. Multibump orbits near the anti-integrable limit for Lagrangian systems. Nonlinearity, 1997;10:1015-1029.

[8] Chen Y-C. Multibump orbits continued from the anti-integrable limit for Lagrangian systems. Regul Chaotic Dyn, 2003;8:243-257.

[9] Chen Y-C. Anti-integrability in scattering billiards. Dynamical Systems, 2004;19:145-159.

[10] Chen Y-C. Anti-integrability for the logistic maps. Preprint.

[11] Chen Y-C. Bernoulli shift for second order recurrence relations near the anti-integrable limit. Discrete Contin Dyn Syst B, 2005;5:587-598.

[12] Aubry S. Anti-integrability in dynamical and variational problems. Physica D, 1995;86:284-296.

[13] Hénon M. A two-dimensional mapping with a strange attractor. Comm Math Phys, 1976;50:69-77.

[14] Hao B-L. Chaos. Singapore: World Scientific, 1984.

[15] Murakami C, Murakami W and Hirose K. Sequence of global period doubling bifurcation in the Hénon maps. Chaos Solitons Fractals, 2002;14:1-17.

[16] Devaney RL and Nitecki Z. Shift automorphisms in the Hénon mapping. Comm Math Phys, 1979;67:137-146.

[17] Sterling D and Meiss JD. Computing periodic orbits using the anti-integrable limit. Phys Lett A, 1998;241:46-52.

[18] Aziz-Alaoui MA, Robert C and Grebogi C. Dynamics of a Hénon-Lozi-type map. Chaos Solitons Fractals, 2001;12:2323-2341.

[19] Banks J and Dragan V. Smale's horseshoe map via ternary numbers. SIAM Rev, 1994;36(2):265-271.

[20] Robinson C. Dynamical Systems - Stability, Symbolic Dynamics, and Chaos. London: CRC Press, 1995.

[21] Wiggins S. Introduction to Applied Nonlinear Dynamical Systems and Chaos. 2nd Edition. New York: Springer-Verlag, 2003.

[22] Guckenheimer J and Holmes P. Nonlinear Oscillations, Dynamical Systems, and Bifurcations of Vector Fields. London: Springer-Verlag, 1983.

[23] Sprows D. Digitally determined periodic points. Math Mag, 1998;71:304-305.